Electronic Supplementary Material (ESI) for Journal of Materials Chemistry A.

Supporting Information

Following carbon condensation by in-situ TEM: Towards a rational understanding of the processes in the synthesis of nitrogen-doped carbonaceous materials

D. Piankova et al.

Experimental

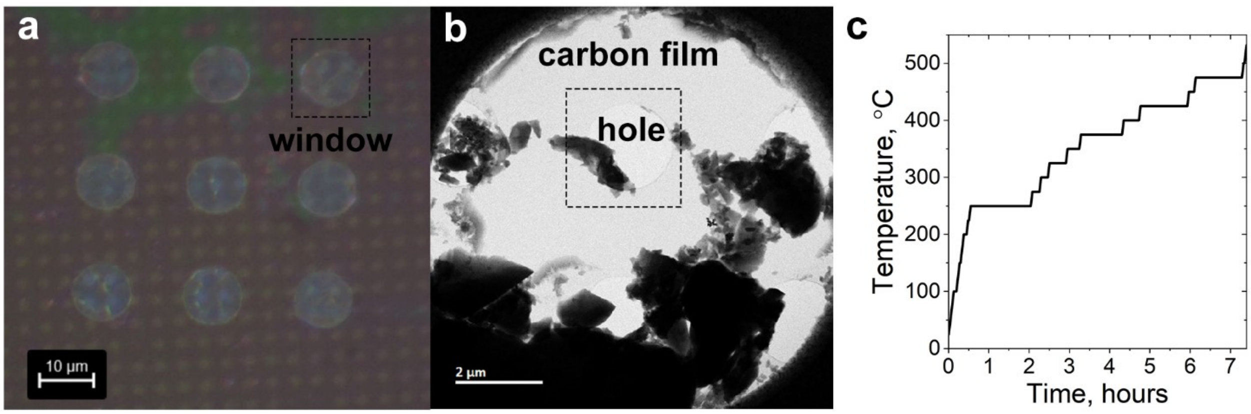

Fig. S1. a) light microscopy image of the the heating chip window; 2) enlargement of the window showing the overview of the deposited sample before the heating, recorded in STEM using SE and BF detector. Heating ramp for the in-situ STEM heating experiment

1. *Characterization of the precursor*

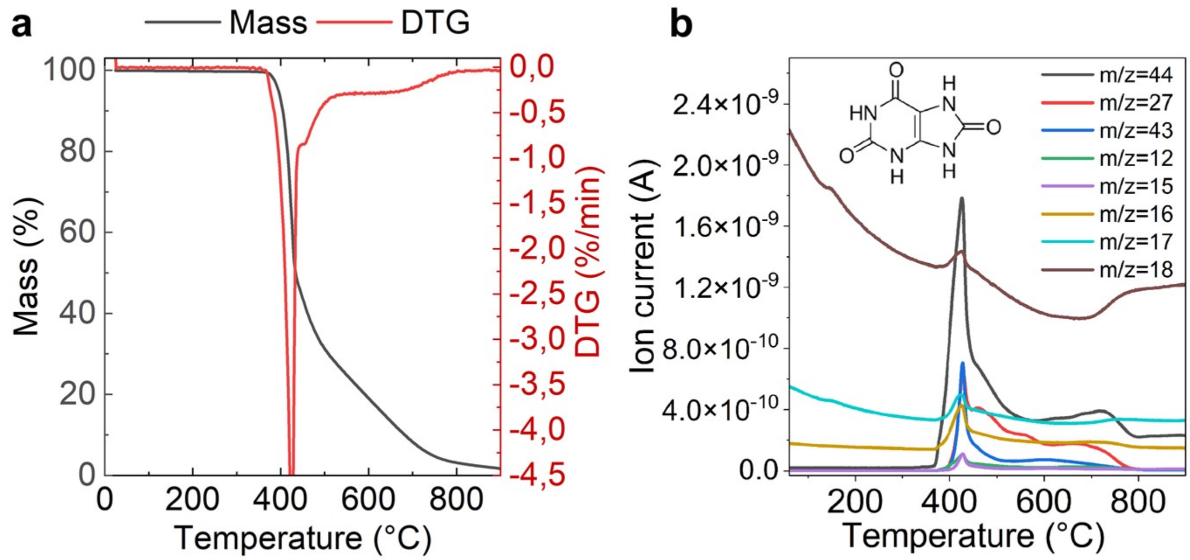

Fig. S2. a) TGA of uric acid in nitrogen atmosphere, b) TGA-MS results of uric acid in nitrogen atmosphere, possibly ascribed signals m/z=44: CO_2^+, $N_2O^+CN_2H_4^+$, $CNOH_2^+$, $C_2H_4O^+$, m/z=27: HCN^+, m/z=43: $CNOH^+$, $CN_2H_3^+$, $C_2NH_5^+$, $C_2OH_3^+$, m/z=12: C^+, m/z=15: CH_3^+, NH^+, m/z=16: O^+, NH_2^+, CH_4^+, m/z=17: OH^+, NH_3^+, m/z=18: H_2O^+.

2. *Synthesis in nitrogen atmosphere*

Table S1. The samples used in the manuscript.

Sample name UA"temperature"-"gas"-"heating rate"	temperature [°C]	atmosphere	pressure [bar]	heating rate [K/min]
UA500-N_2-1	500	nitrogen	1	1
UA700-N_2-1	700	nitrogen	1	1
UA800-N_2-1	800	nitrogen	1	1
UA400-vac-1	400	vacuum	$1.5*10^{-4}$	1
UA500-vac-1	500	vacuum	$1.5*10^{-4}$	1
UA500-vac-10	500	vacuum	$1.5*10^{-4}$	10

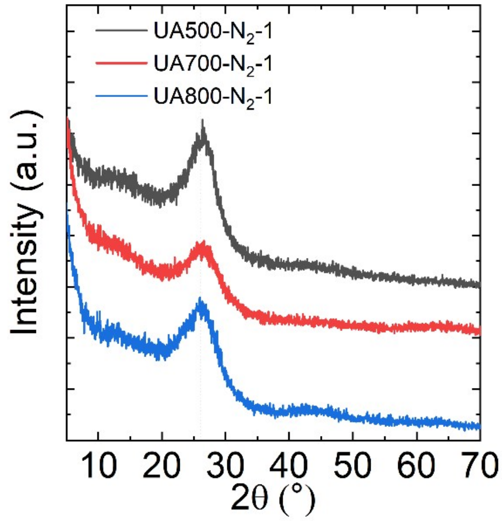

Fig. S3. XRD pattern of UA500-N_2-1, UA700-N_2-1, and UA800-N_2-1.

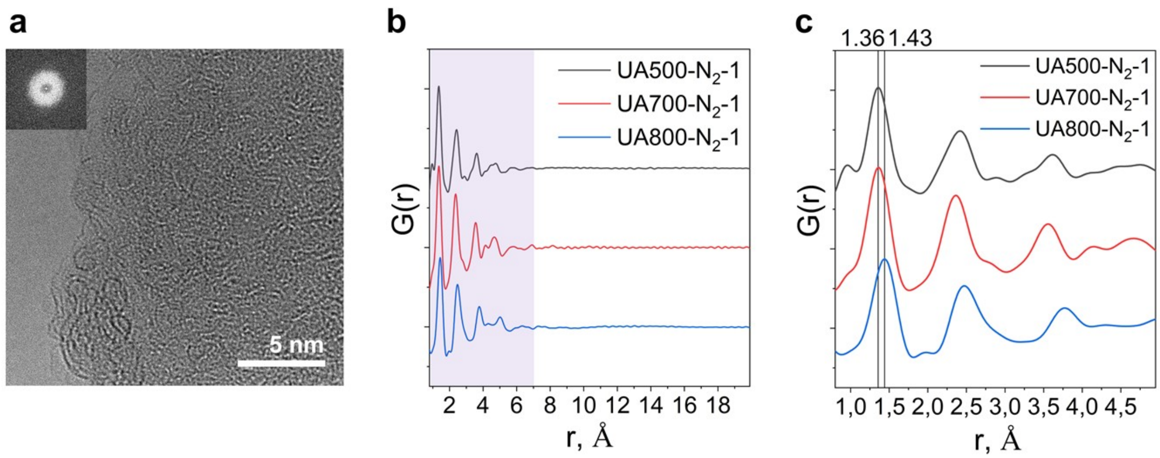

Fig. S4. a) HRTEM and FFT transform (inset) of the corresponding area of the sample UA700-N_2-1; eRDF (electron reduced density function) analysis of the samples synthesized at 500,700 and 800 °C in nitrogen atmosphere: b) EF-eRDFs, purple rectangular shows the region where the short-range order is present c) enlargement of the short-range order.

The point of the extinction of the peaks in EF-eRDF shows the length of the short-range order (**Fig. S4 b**), which is approximately 7 Å for all the materials. To get quantitative information about bonding in the short-range order, we analyzed the peak positions in the eRDF. The first neighbor-neighbor distance for the sample UA500-N_2-1 and UA700-N_2-1 is 1.36 Å, which is shorter in contrast to the UA800-N_2-1 sample, where the distance is 1.42-1.43 Å, corresponding to the typical carbon-carbon distance in amorphous carbonaceous materials[1]. Shorter distances in the first coordination sphere indicate the presence of mostly carbon-nitrogen bonds in the network. These findings go along with the compositional analysis: samples UA500-N_2-1 and UA700-N_2-1 demonstrate higher nitrogen content than UA800-N_2-1 (**Table 1**). Thus, EF-eRDF analysis showed that the samples demonstrate the same length of short-range order of 7 Å with the only difference in the first neighbor-neighbor distance arising from the difference in the composition.

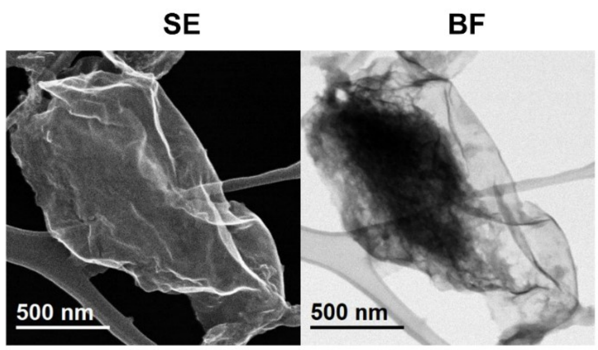

Fig. S5. Secondary electron (SE) and bright-field (BF) STEM images of the sample UA800-N_2-1.

3. *In-situ scanning transmission electron microscopy*

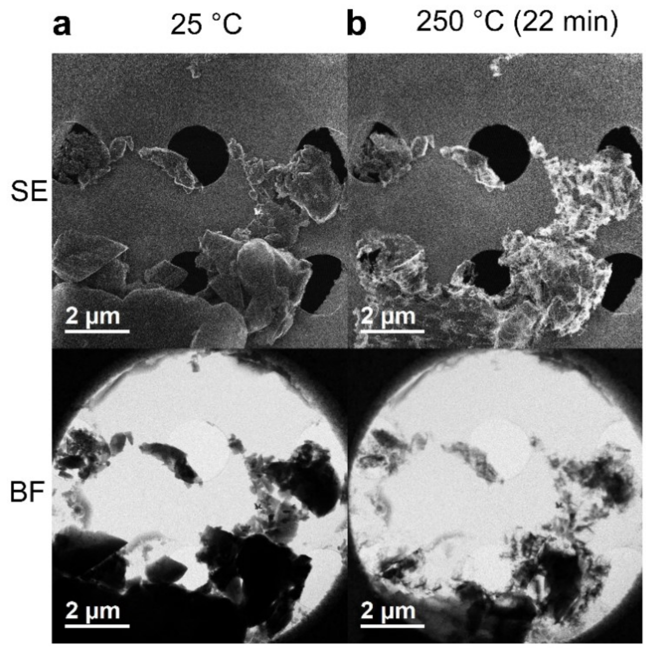

Fig. S6. Secondary electron and bright-field STEM images of: a) specimen before the in-situ heating experiment, b) at 250 °C after isothermal heating for 22 minutes.

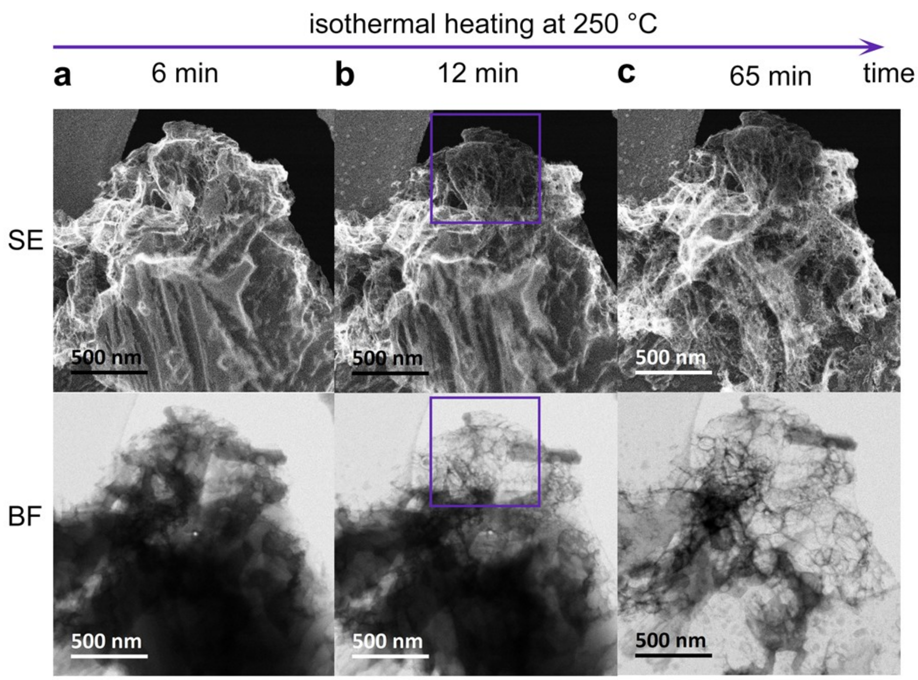

Fig. S7. Secondary Electron and bright-field STEM images of the particle during the isothermal heating at 250 °C a) after 6 minutes; b) after 12 minutes (the area in the rectangular was imaged at higher magnification); c) after 65 minutes. The particle got emptied faster in the imaged area of interest (b –

in rectangular), however, after isothermal heating for 65 minutes without any exposure to the electron beam particle looked emptied in almost all the areas.

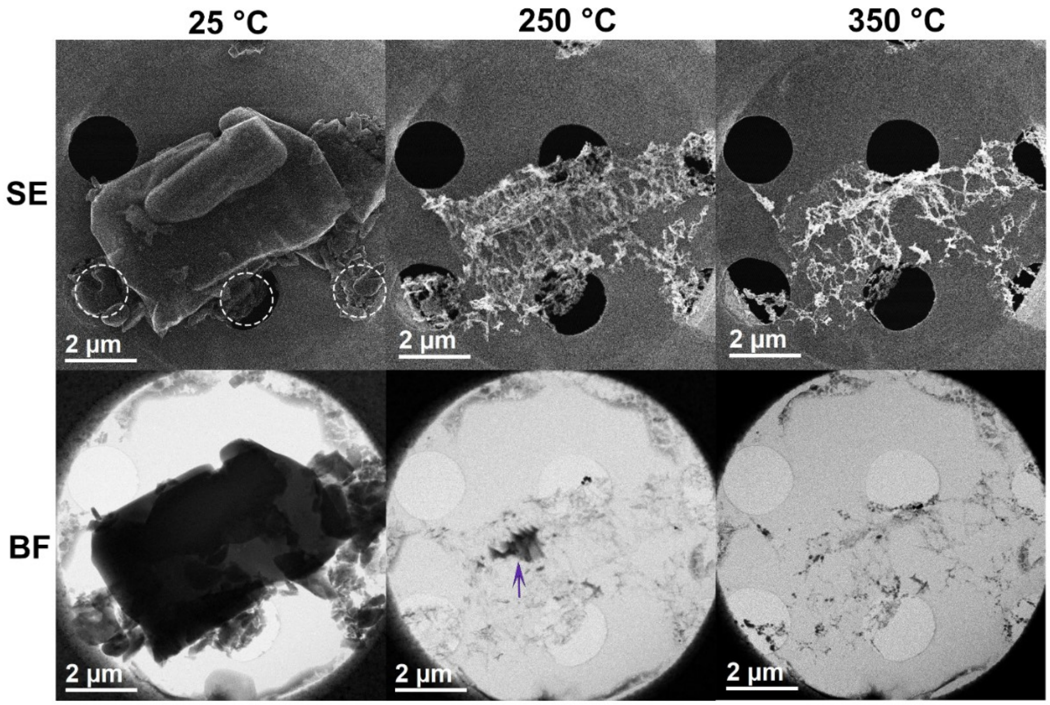

Fig. S8. Secondary Electron and bright-field STEM images of the shrinkage of particles from 25 to 350 °C. The small particles shown in white dotted circles (SE STEM image at 25 °C) slightly shrank from 25 to 250 °C and more considerably from 250 to 350 °C.

4. Optimization of the synthesis using vacuum

Table S2. Samples synthesized in vacuum to determine the condensation temperature.

Sample name UA"temperature"-"gas"-"heating rate"	**temperature [°C]**	**atmosphere**	**pressure [bar]**	**heating rate [K/min]**
UA250-vac-10	250	vacuum	$1.5*10^{-4}$	10
UA325-vac-10	325	vacuum	$1.5*10^{-4}$	10
UA375-vac-10	375	vacuum	$1.5*10^{-4}$	10
UA500-vac-10	500	vacuum	$1.5*10^{-4}$	10

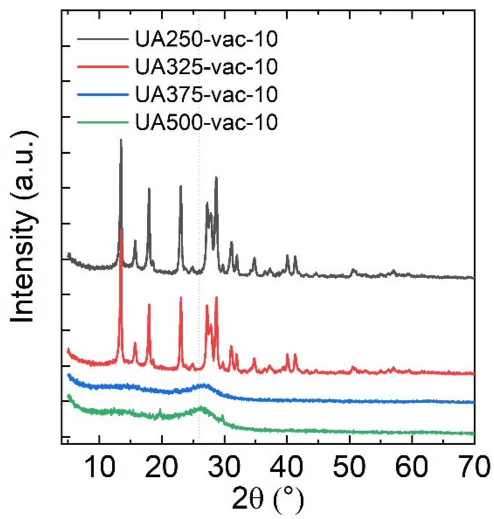

Fig. S9. Determination of the condensation temperature in vacuum by XRD.

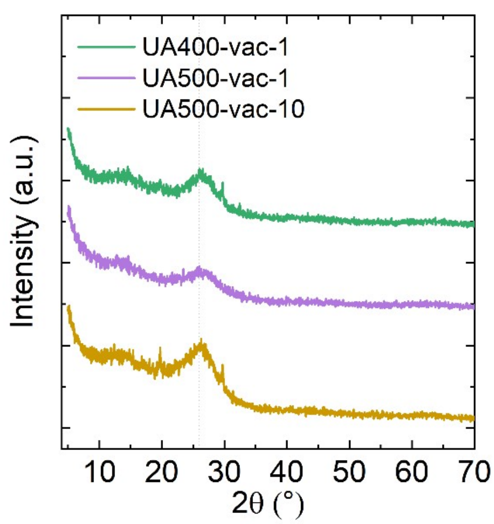

Fig. S10. XRD of the samples carbonized in vacuum.

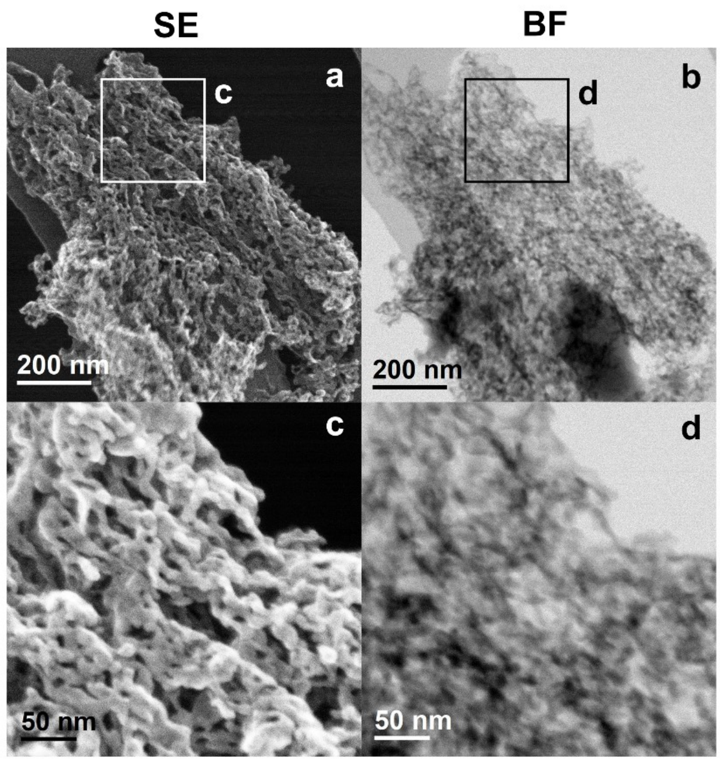

Fig. S11. Secondary electron (SE) and bright-field images (BF) of the sample UA400-vac-1.

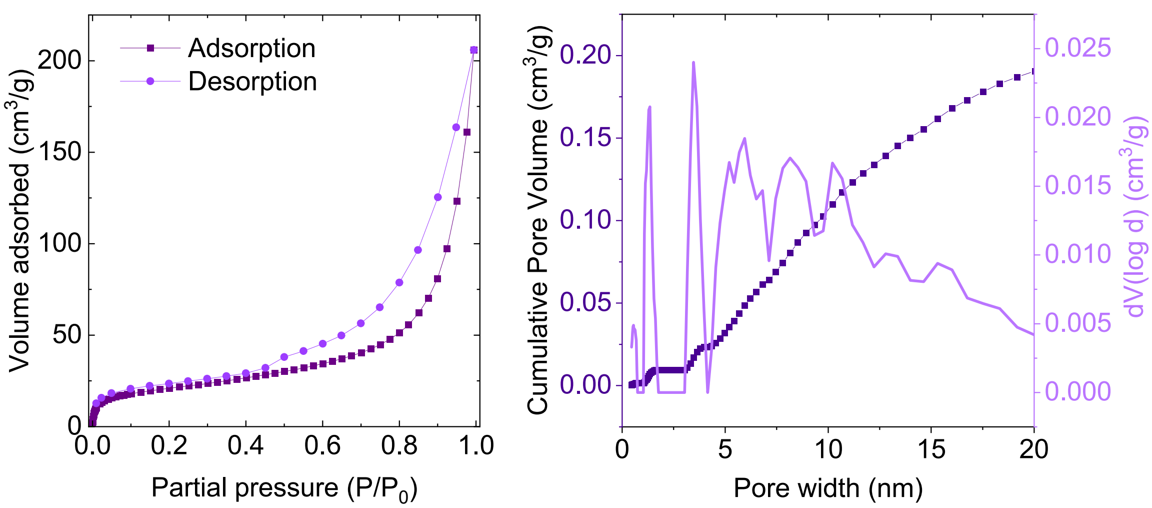

Figure S12. (Left) Ar adsorption/desorption isotherm recorded at 87K and (right) NLDFT pore size distribution obtained by applying the kernel to the adsorption branch (slit pores) of UA500-vac-1.

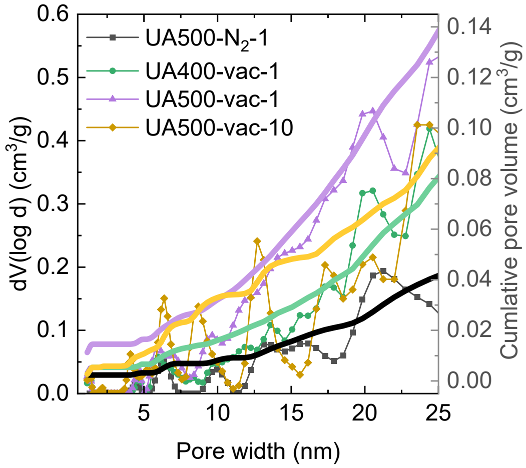

Figure S13. Pore size distribution of samples UA500-N_2-1, UA400-vac-1, UA500-vac-1, and UA500-vac-10 obtained by applying the NLDFT (slit pore pores) to the adsorption branch of N_2 adsorption/desorption isotherms at 77K.

5. Selectivity and heat of adsorption

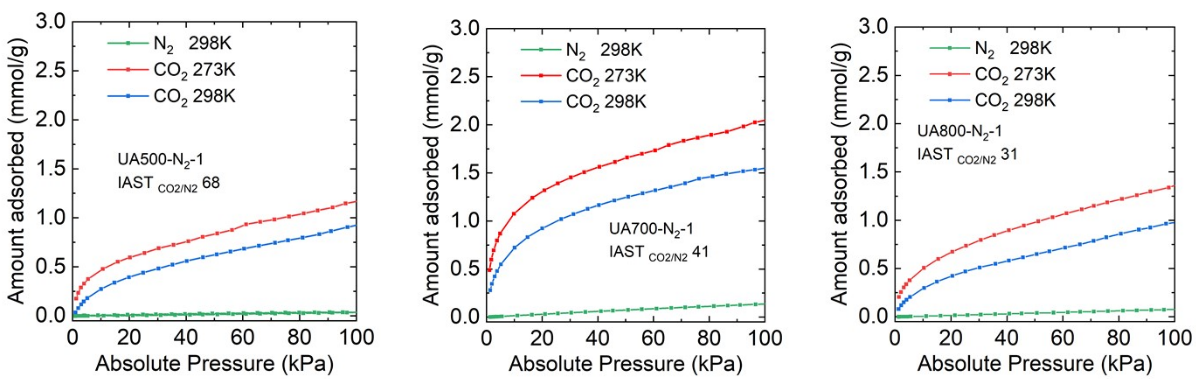

Fig. S14. IAST values calculated from CO_2 and nitrogen adsorption isotherms at 298 K of samples prepared in nitrogen atmosphere.

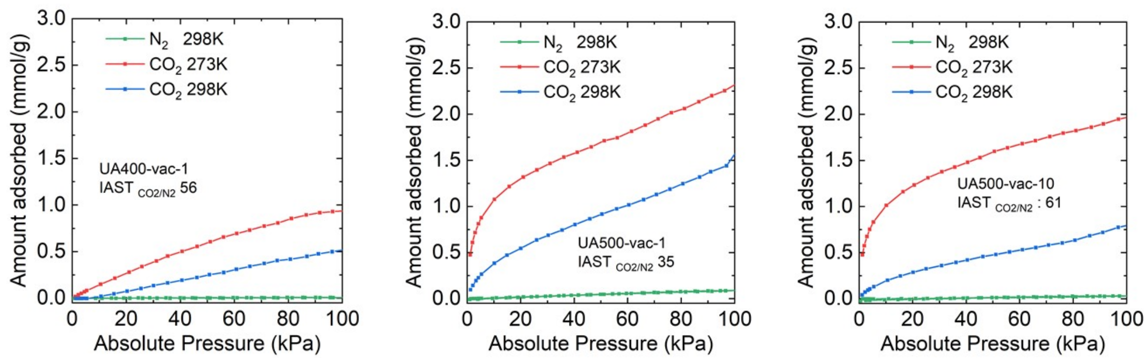

Fig. S15. IAST values calculated from isotherms vacuum samples.

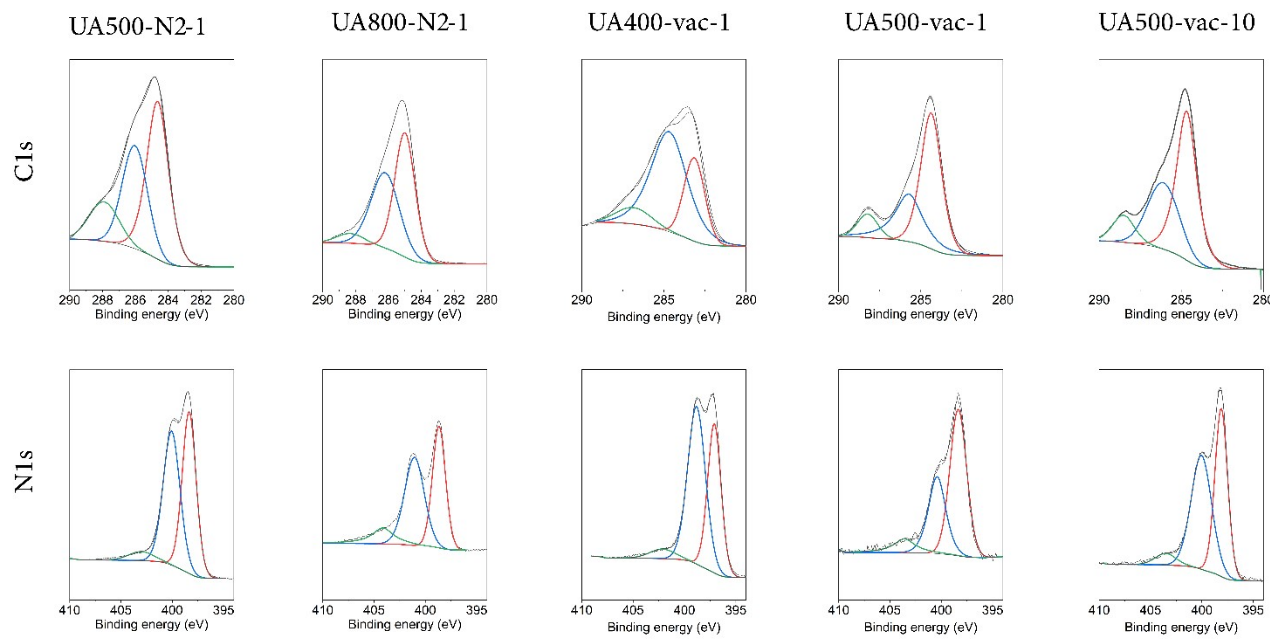

Fig. S16. Deconvoluted C1s and N1s XPS spectra. Pyridinic nitrogen is shown in red, pyrrolic - in blue, and quaternary - in green.

References

1 V. Petkov, R. G. Difrancesco, S. J. L., *Philosophical Magazine B*, 1999, **79**, 1519–1530.